water

MDPI

Article

Impacts of Land-Use Types and Landscape Patterns on River Water Quality in the Dry-Hot Valley Basin with Frequent Geological Hazards in the Southwest China

Honglei Tang [1], Jiangwen Yang [1], Chunyu Yang [2], Songpei Li [2], Liang Qi [2], Linxuan Zhou [1], Chenjue Tong [1], Haonan Ren [1] and Yifei Yang [1,3,*]

[1] Faculty of Electric Power Engineering, Kunming University of Science and Technology, Kunming 650500, China; tanghonglei@kust.edu.cn (H.T.); jwyang0725@163.com (J.Y.)
[2] Huadian Jinsha River Midstream Hydropower Developmeng Co., Ltd., Kunming 650500, China
[3] Xinjiang Uygur Autonomous Region Rivers and Lakes Protection Center, Urumqi 830000, China
* Correspondence: y1620365043@163.com

Abstract

Under the intensifying pressures of climate change and human activities, the characteristics of land-use types and landscape patterns are widely recognized to exert significant influences on river water quality. Nevertheless, in dry-hot valley basins characterized by fragile ecological conditions and frequent geological hazards, the responses of river water quality to changes in landscape characteristics under the combined effects of natural disasters and anthropogenic disturbances remain poorly understood. In the present study, the Xiaojiang River Basin, a typical dry-hot valley basin subjected to intensive anthropogenic activities and frequent geological hazards, was selected. Through the integration of landscape pattern indices analysis and redundancy analysis, the spatial and temporal variations in river water quality in the Xiaojiang River Basin were quantified, and the effects of land-use types and landscape patterns on river water quality were systematically elucidated. Results showed that (1) the key water quality indexes such as total phosphorus, total nitrogen, ammonia nitrogen and COD in the Xiaojiang River Basin were shown as flood season > non-flood season; for example, the average TN increased from 1.37 mg/L (non-flood season) to 2.90 mg/L (flood season), and the average COD increased from 3.24 mg/L to 15.98 mg/L. In contrast, DO decreased from 8.07 mg/L (non-flood season) to 6.72 mg/L (flood season), and conductivity decreased from 561.4 μs/cm to 480.90 μs/cm. (2) Spatially, these key water quality indicators were shown as hazard-prone area > residential area > cultivated land area. (3) The larger the area of the debris flow trace areas, the greater the fluxes of nitrogen and phosphorus in the tributaries and the main stream in the flood season, and the worse the water quality of the river; after heavy rainfall, the fluxes of key water quality indicators generally showed a geometric multiple increase, with average growth rates of 1.95 (TP), 2.41 (TN), 2.34 (NH_3-N) and 4.74 (COD), respectively. (4) The ability of landscape patterns in flood season to explain the change in water quality is better than that in non-flood season. On different spatial scales, in the down-stream hazard-prone areas, upstream residential areas and cultivated land areas, the changes in river water quality indicators were mainly affected by landscape pattern indicators such as PD_hazard-influenced areas, IJI_residential areas and DIV_cultivated land. Our results can provide scientific guidance for the soil and water conservation practice, ecological restoration, and land-use management in the dry-hot valley of Southwest China and the water environment protection of the Baihetan Reservoir area.

Check for updates

Academic Editor: Richard Smardon

Received: 15 January 2026
Revised: 9 February 2026
Accepted: 13 February 2026
Published: 27 February 2026

Copyright: © 2026 by the authors. Licensee MDPI, Basel, Switzerland. This article is an open access article distributed under the terms and conditions of the Creative Commons Attribution (CC BY) license.

Keywords: dry-hot valleys; land-use types; landscape pattern; debris flow trace areas; river water quality

1. Introduction

Human activities have altered underlying surface conditions and river systems across multiple temporal and spatial scales [1–4]. With the intensification of human activities and the increasing frequency of global extreme weather events, water quality has been degraded in many countries and regions, posing a significant threat to aquatic ecosystems [5–10]. The degradation of riverine environments and aquatic ecosystems is primarily driven by both natural and anthropogenic factors. Surface water quality is more strongly influenced by land-use types than by environmental factors [11–14]. At the global scale, water pollution can substantially aggravate "clean-water scarcity": a recent assessment across >10,000 sub-basins reported that 2517 sub-basins already faced severe clean-water scarcity in 2010 when both water quantity and nitrogen pollution were considered, and these hotspot sub-basins covered ~32% of the global land area with ~80% of the total population living there [15]. Moreover, extreme rainfall and flood events can trigger pronounced and rapid water quality shifts; for example, a five-year study reported that the largest change in water quality occurred on the second day after rainfall, and that the altered concentrations of some chemical parameters could persist for an extended period [16–18]. The relationship between landscape structure and river water quality is critical for watershed management [19]. Prior to entering river systems through surface runoff, pollutant migration and transformation are regulated by landscape structure [20]. Landscape structure encompasses structural composition (i.e., land-use types) and spatial configuration (i.e., landscape patterns). Inappropriate configurations of landscape structural composition and spatial patterns may promote nutrient transfer to water bodies [21], exacerbating nonpoint source pollution risks in watersheds [22]. Consequently, elucidating the relationship between landscape structure and river water quality can inform watershed ecological restoration and land-use management.

Landscape ecology defines spatial patterns as the structure, arrangement, and location of objects within any given landscape. As key regulators of watershed nonpoint source pollution, land-use types, composition, and landscape patterns (e.g., patch connectivity and corridor layout) influence pollutant migration pathways and retention efficiency through physical interception, biodegradation, and other processes [23]. Notably, land-use practices, as major drivers of landscape composition, play a significant role in the generation intensity and diffusion path of pollution [24]. Studies have shown that human activities such as mining and waste disposal [25], grazing [26], cropland reclamation [27], and urbanization [28] have exacerbated river water quality deterioration, thereby degrading watershed aquatic environments. For instance, Nafi'Shehab et al. [29] found that the deterioration of the water quality of the Binton River in Malaysia is related to the high proportion of urban and agricultural land-use in the basin and the high patch density of these landscapes. A limited number of studies [30] indicate that adventitious geohazards such as landslides, collapse, debris flows, and other gravitational erosion processes can also significantly alter river water quality characteristics, thereby affecting river aquatic environments to varying degrees. For instance, Le et al. [31] found in their study of Australia's Murray River that the impacts of flood disasters on downstream aquatic environments could persist for up to 32 years. Danehy et al. [32] also demonstrated in their study of rivers in the Cascade Mountains of Oregon, USA, that the effects of debris flows on the aquatic environment may persist for extended periods until the riparian zone of the affected river segment recovers

as mature Alnus rubra forests, which gradually restore damaged aquatic ecosystems by providing nitrogen inputs and shading effects. However, in the fiagile, frequently disaster-prone dry-hot valley watersheds, the response patterns of river water quality to landscape changes caused by the combined effects of natural disasters and human disturbances remain unclear.

The Xiaogjiang River Basin in Yunnan Province is located in the lower reaches of the Jinsha River and exhibits a typical dry-hot valley climate [33]. Precipitation within the basin is concentrated, and droughts are severe. Once vegetation is destroyed, it is difficult to restore. Furthermore, the river channels within the basin developed along fault zones and the rock strata are fragmented, resulting in poor erosion resistance. Consequently, soil erosion is extremely severe [34]. Over the past century, human activities such as mining and waste disposal, excessive deforestation, steep slope cultivation, and overgrazing have intensified water and soil loss and ecological degradation in the Xiaojiang Basin [35]. Furthermore, landslides and debris flows are widespread and frequent in the Xiaojiang basin. Statistics indicate 107 debris flow channels along both banks of the Xiaojiang River, discharging approximately 2.6 million tons of sediment into the Jinsha River during annual flood seasons. The above reasons have led to a large amount of dissolved and adsorbed nitrogen and phosphorus pollutants flowing into the main channel of the Xiaojiang River in a short period of time, along with heavy rain floods and debris flow disasters, and being transported to the main stream of the Jinsha River. On the other hand, the advantages of light and heat resources in the dry-hot valley basins have led to the rapid development of river valley agriculture and the acceleration of urbanization in the Xiaojiang River Basin [36], while the man-made pollution of river water quality is also intensifying. These factors may contribute to the Xiaojiang River Basin becoming one of the important sources of nitrogen and phosphorus pollutants in the Baihetan Reservoir [37]. However, as the main tributary of the Baihetan Hydropower Station Reservoir area, the second largest hydropower station in China, the Xiaojiang River Basin remains unclear in terms of the temporal and spatial characteristics of water quality changes under the dual influence of natural disasters and human activities.

The Xiaojiang River Basin, a typical dry-hot valley basin characterized by intensive anthropogenic activities and frequent geological hazards, was selected as the study area, where systematic monitoring of water and sediment quality was conducted. By integrating landscape pattern indices analysis based on Fragstats 4.2 and redundancy analysis, the spatial and temporal variations in river water quality in both the main stream and tributaries of the Xiaojiang River Basin were quantified, and the impacts of land-use types and landscape patterns on river water quality under the combined effects of intensive anthropogenic activities and geological hazards were clarified. The results of this study can provide scientific guidance for soil and water conservation, ecological restoration, land-use management in the dry-hot valleys of Southwest China, and water environment protection in the Baihetan Reservoir area.

2. Materials and Methods

2.1. Study Area and Sampling

The Xiaojiang River originates from the Yuwei Back Mountain in Xundian County, Yunnan Province. It flows from south to north through Xundian County and Dongchuan District of Kunming City and Huize County of Qujing City, and finally joins the Jinsha River. Xiaojiang is a first-level tributary on the right bank of the Jinsha River in the upper reaches of the Yangtze River. Its main channel is 141.93 km long, and its drainage area is 3058.98 square kilometers. The Xiaojiang River Basin belongs to the high-to-medium mountain canyon landform type of the Yunnan-Guizhou Plateau, with

an overall south-high, north-low elevation gradient ranging from 691.00 to 4289.00 m (Figure 1a). The upper reaches of the Xiaojiang River Basin are located in the plateau mountain monsoon climate zone, while the lower reaches are in the typical dry-hot river valley zone [38], characterized by a semi-arid subtropical climate [35], with an average annual precipitation of 694.00 to 1400.00 mm and an average annual potential evaporation of 1570.00 to 2180.00 mm. The Xiaojiang River Basin has distinct rainfall seasons and concentrated precipitation. Approximately 88% of the precipitation occurs from April to October, and 50% occurs from June to August. Owing to the large altitude difference, significant variations in temperature with altitude, and uneven temporal and spatial distribution of precipitation, the vertical differentiation of vegetation, soil, and land-use within the basin is evident. In addition, mining and waste disposal, excessive deforestation, steep slope cultivation, and overgrazing have had a severe impact, resulting in a complex landscape pattern within the Xiaojiang River Basin. Moreover, the Xiaojiang River Basin is squeezed by the Hengduan Mountains and the Yunnan-Guizhou Plateau, featuring active tectonics, frequent earthquakes, and abundant loose material sources. This has led to frequent landslides and debris flows induced by heavy rain [39], further exacerbating the fragmentation of the basin landscape pattern.

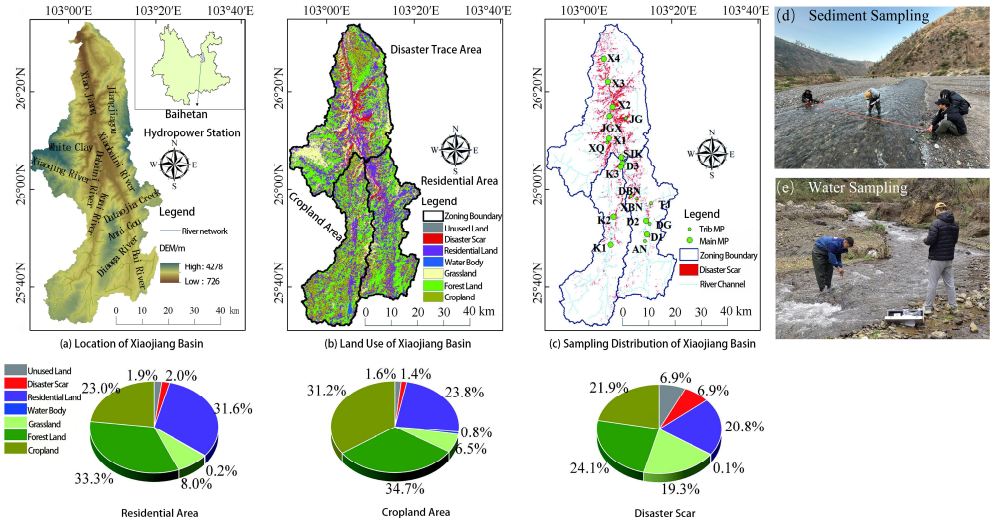


Figure 1. Overview of the Xiaojiang River Basin.

To characterize the spatial heterogeneity and event-scale responses of water–sediment–water quality in the Xiaojiang River Basin under contrasting land-use settings and hazard disturbances, we designed a basin-wide monitoring network based on (1) the spatial differences in land-use proportions among characteristic zones, (2) the distribution of landslide and debris-flow hazard-influenced areas, (3) field accessibility and sampling safety, and (4) the principle of full watershed coverage and hydrological connectivity. According to the spatial differences in the proportion of land-use in the Xiaojiang River Basin, the basin was divided into three characteristic zones (Figure 1b): the upstream cultivated land area (Kuai River Basin; highest proportion of cultivated land), the upstream residential area (Dabai River Basin; highest proportion of urban land), and the downstream hazard-prone area (lower reaches of Xiaojiang River Basin; relatively high proportion of landslide and debris flow hazard-influenced area). The monitoring sites were arranged to ensure both zonal representativeness and longitudinal coverage along the river network. Specifically, along the two major upstream main streams—the Dabai River (east) and the Kuai River (west)—three sampling points were established on the upper, middle, and lower reaches of each main stream to capture longitudinal gradients within the upstream zones. From the confluence of the Dabai River and the Kuai River to the downstream main stem

of the Xiaojiang River, four sampling points were further arranged along the course to characterize mixing at confluences and downstream accumulation processes. The outlet site of the Xiaojiang River Basin was located in the tailwater area of the Baihetan Reservoir. In addition, considering that landslides and debris flows can generate pulsed inputs of sediment and associated pollutants during the flood season, seven branch gullies with frequent landslide and debris-flow activity were included based on historical records and field surveys: Anni Gully (AN), Diao Ga River (DG), Tao Jia Small River (TJ), Xiao Bai Ni Gully (XBN), Da Bai Ni Gully (DBN), Xiao Qing River (XQ), and Jiang Jia Gully (JG). Overall, this design included 10 sampling points on the main stem and 7 points on the tributaries/branch gullies (Figure 1c), providing systematic coverage of the cultivated-land zone, residential zone, and hazard-prone zone, as well as the main stem–tributary network and key confluence/outlet control sections.

The sampling strategy combined seasonal synoptic sampling with rainfall-event process sampling. Basin-wide sampling campaigns were conducted in December 2023, January 2024, and April 2024 (non-flood season), as well as June and August 2024 (flood season). In addition, a one-week continuous monitoring campaign was conducted in August 2024, during which water–sediment–water quality changes before and after each rainstorm were compared to quantify event-driven perturbations and potential lagged responses. In total, 128 water samples were collected in this study. During sampling, pH, electrical conductivity, dissolved oxygen, and temperature were measured in situ using the Tianer Portable Water Quality Analyzer (TE-700Plus; Tianer Analysis Instruments (Tianjin) Co., Ltd., Tianjin, China). Water samples were sealed in polyethylene bottles, stored at 4 °C, and transported under the same temperature-controlled conditions. After filtration through a 0.45 μm membrane in the laboratory, total phosphorus (TP), total nitrogen (TN), total ammonia nitrogen (NH_3-N), and chemical oxygen demand (COD) were determined by ammonium molybdate spectrophotometry, the alkaline potassium persulfate method, Nessler's reagent spectrophotometry, and rapid digestion spectrophotometry, respectively. In parallel, river water depth was measured using a standard water gauge, and the mean depth at each sampling point was calculated as the average of three measurements. Flow velocity was measured at one-third of the water depth below the surface using a Leistar portable flowmeter (LS1206B; Jiangsu Tongda Instrument Co., Ltd., Huai'an, Jiangsu, China), and channel width at each sampling point was measured with a laser rangefinder. Discharge at each sampling point was calculated based on the water depth, flow velocity, and channel width derived from the three-point hydrological measurements. A 1 L sediment-containing water sample was collected at each sampling point; after pretreatment, the sample was dried and weighed to determine sediment content, yielding sediment concentration data for the river water.

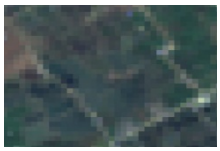
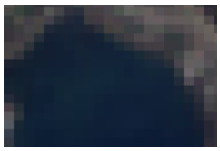
2.2. Research Methods

2.2.1. Land-Use Analysis and Debris Flow Trace Areas

The Landsat8 OLI 30 m satellite remote sensing data of the Xiaojiang Basin with cloud cover below 5% in 2023 were downloaded from the Geospatial Data Cloud Platform of the Chinese Academy of Sciences. After undergoing radiometric, atmospheric, and geometric corrections using ENVI 5.0 software, the 2023 land-use data for the Xiaojiang River Basin were obtained. During the interpretation process, the maximum likelihood method was adopted for supervised classification. Training areas were established based on historical records and interpretation markers set up through field investigations, yielding preliminary classification results [40]. Based on this, combined with manual visual interpretation and further correction, the land-use map of the Xiaojiang River Basin in 2023 was obtained [41]. As shown in Figure 1b, the land-use types in the Xiaojiang River Basin were mainly

classified as forest land (28.67%), cultivated land (25.93%), urban land (24.58%), grassland (12.50%), landslide and debris flow sites (4.01%), unutilized land (3.96%), and water areas (0.35%) (Table 1).

Table 1. Land-use interpretation and image.

Category	Definition	Field Footage	ENVI Imagery	Google Earth Imagery
Arable land	Land used for agricultural production, cultivated and suitable for growing crops.			
Woodland	Forested land is defined as areas covered by vegetation such as trees, bamboo, and shrubs.			
Grassland	Grassland is defined as an area covered by herbaceous plants with a growth coverage of 5% or more.			
water area	Refers to areas covered by water bodies, including natural or artificial bodies of water such as lakes, rivers, and ponds.			
Residential land	Land designated for human habitation and related activities, including residential areas, public facilities, and commercial zones.			
Debris flow trace areas	Disaster-affected sites refer to land that has experienced natural disasters and has not been significantly disturbed by human activity.			
Unutilized land	Land in its natural state that has not yet been developed, cultivated, or built upon.			

Note: Reference imagery was obtained from Google Earth (Image © Google, accessed in October 2025) and was used for visual interpretation and sample verification.

2.2.2. Calculation of Pollutant Flux and Sediment Transport Rate

Pollutant flux refers to the total mass of a given pollutant passing through a specific site (cross-section) per unit time, reflecting the combined effects of hydrological, geological, chemical, and biological processes in the aquatic environment. The pollutant flux was calculated as

$$F = C \times Q \times 10^{-3} \quad (1)$$

where F is the pollutant flux (kg s^{-1}), C is the pollutant concentration at the monitoring site (mg L^{-1}), and Q is the cross-sectional discharge at the monitoring site (m^3 s^{-1}). The factor 10^{-3} converts mg L^{-1} × m^3 s^{-1} to kg s^{-1}.

In addition, the sediment transport rate in this study refers to the suspended sediment flux (kg s^{-1}), the mass of suspended sediment passing through the cross-section per unit time. It was calculated using the same framework:

$$F_s = SSC \times Q \times 10^{-3} \quad (2)$$

where F_s is the sediment transport rate (suspended sediment flux, kg s^{-1}), SSC is the suspended sediment concentration (mg L^{-1}), and Q is the cross-sectional discharge (m^3 s^{-1}).

2.2.3. Landscape Pattern Analysis of the Basin

To further quantify landscape pattern characteristics in the Xiaojiang River Basin, seven widely applicable landscape indices were selected from those characterizing landscape density, area, fragmentation, aggregation, connectivity, and diversity (Table 2). These include patch density (PD), largest patch index (LPI), total patch area (CA), separation index (SPLIT), aggregation index (AI), landscape-scale spread index (CONTAG), and Shannon diversity index (SHDI). These indices were calculated using Fragstats 4.2 software.

Table 2. Description of landscape pattern indexes used in this study [42–45].

Landscape Index	Scale	Computation Formula	Description
Patch Density	Type	$PD = \frac{n_i}{A} \times 1000000$	Number of patches per unit area
Largest patch index	Type	$LPI = \frac{max_{j=1}^{n}(a_{\{ij\}})}{A} \times 100$	The percentage of the largest patch in the total landscape
Total (Class) Area	Type	$CA = \sum_{j=1}^{n} a_j(\frac{1}{10000})$	Total area by type
Splitting Index	Type	$SPLIT = \frac{A^2}{\sum_{j=1}^{n} a_j{}^2}$	Ratio of the sum of squares of the total landscape area to the sum of squares of the patch area, and the degree of separation of different patch individuals within the landscape type (%)
Aggregation Index	Type	$AI = [\frac{g_j}{max \to g_j}](100)$	The number of similar adjacents involving the corresponding class (%)
Contagion Index	Landscape	$CONTAG = [1 + \frac{\sum_{i=1}^{m}\sum_{k=1}^{m}\left[p_i \frac{g_{ik}}{\sum_{k=1}^{m} g_{ik}}\right]\left[\ln\left(p_i \frac{g_{ik}}{\sum_{k=1}^{m} g_{ik}}\right)\right]}{2\ln(m)}](100)$	Reflect the aggregation degree or extension trend of different plaque types
Shannon's diversity Index	Landscape	$SHDI = -\sum_{i=1}^{n}(p_i ln p_i)$	Reflects landscape heterogeneity

Note: n = The number of patches in the patch type (class) landscape, A = the area (m^2) of the entire landscape, aij = the area (m^2) of patch ij, max-gij = the maximum number of similar adjacencies (connections) between pixels of patch type (class) i based on the single count method, gik = the number of adjacency (connection) between the pixels of patch type (class) i and k based on the double counting method, pi = the proportion of the area of patch type (class) i to the landscape area.

Landscape patterns affect river water quality at sampling points on a certain spatial scale by mediating processes such as rainfall production and runoff, mountain-river hydrological response, and solute transport. This study selected two typical spatial scales, namely the sub-basin and the 1000 m riverbank buffer zone, to quantitatively study the influence of the landscape pattern characteristics of the Xiaojiang River Basin on the water quality of the river. Based on the 30 × 30 m resolution Digital Elevation Model (DEM) of the Xiaojiang River Basin in 2023, with each water quality sampling point as the outlet of the sub-basin, the Xiaojiang River Basin was divided into 10 sub-basin buffer zones using ArcSWAT 10.6 software to investigate the influence of the landscape pattern within the sub-basin buffer zones on the water quality of the river. Field surveys revealed that the average width of the riparian zone in the Xiaojang River Basin is approximately 1000 m. Therefore, using the river network of the Xiaojiang River Basin extracted by ArcGIS 10.6 software, taking the cross-section of each water quality monitoring point as the benchmark, a riverbank buffer zone was established with a length parallel to the river channel and

extending upstream to the water quality monitoring point at the outlet of the Shangyouzi River Basin, and a width of 1000 m perpendicular to both banks of the river channel. This study investigated the impact of riparian landscape patterns on river water quality.

2.2.4. Data Analysis

Redundancy Analysis is a constrained ranking of Principal Component Analysis (PCA), which is used for multivariate statistical analysis involving multiple explanatory and response variables. This study adopted Redundancy Analysis (RDA) to test the positive and negative correlations between various landscape pattern indicators and water quality indicators at different scales, quantifying their interpretation and contribution rates to the changes in water quality indicators. Eight water quality indicators of 17 water quality monitoring points in the Xiaojiang River Basin during the flood and non-flood seasons were taken as response variables, and seven landscape pattern indices were taken as explanatory variables in RDA across two typical spatial scales, and 999 Monte Carlo permutation tests were used to test the significance level of the explanatory variables. The influence of landscape indices on water quality at each scale was screened by selecting the preceding items in the redundant analysis. By analyzing the significant variables and the interpretation rate of water quality changes [46], the interpretation rate and contribution rate of landscape pattern indicators to water quality indicators at different spatial scales were ultimately obtained [40]. All statistical analyses were completed in Canoco 5.0 software.

3. Results

3.1. Spatio-Temporal Distribution of Water Quality in the Xiaojiang River Basin

3.1.1. Temporal Distribution of Water Quality Indicators

Figure 2 illustrates the temporal distribution characteristics of water quality indicators such as total phosphorus, total nitrogen, ammonia nitrogen, chemical oxygen demand (COD), and temperature in the Xiaojiang River Basin. The average watershed values of total phosphorus, total nitrogen, ammonia nitrogen, COD, and temperature indicators showed the trend of flood period > non-water season. For example, the average values of total nitrogen index during the flood season and non-flood season were 2.90 mg/L and 1.37 mg/L, respectively; the average values of COD index during the flood season and non-flood season were 15.98 mg/L and 3.24 mg/L, respectively. Indicators such as dissolved oxygen and conductivity exhibited a characteristic of lower values during the flood season than during the non-flood season. The average values of the dissolved oxygen index during the flood season and the non-flood season were 6.72 mg/L and 8.07 mg/L, respectively. The average values of the conductivity index during the flood and non-flood seasons were 480.90 μs/cm and 561.4 μs/cm, respectively.

Data for indicators such as total phosphorus, total nitrogen, ammonia nitrogen, and chemical oxygen demand (COD) also showed significant differences between the non-flood and flood seasons. For example, the mean COD concentration was 11.16 mg/L, and the proportion of sampling sites with COD values of 0–11.16 mg/L decreased from 98.0% in the non-flood season to 43.5% in the flood season. The mean TN concentration was 2.12 mg/L, and the proportion of sampling sites with TN values of 0–2.12 mg/L declined from 80.0% in the non-flood season to 47.8% in the flood season. In contrast, dissolved oxygen (DO) and pH exhibited the opposite trend: the mean DO concentration was 7.42 mg/L, and the proportion of sampling sites with DO values of 0–7.42 mg/L decreased from 93.48% in the flood season to 80.00% in the non-flood season; the mean pH was 8.34, and the proportion of sampling sites with pH values of 7.00–8.34 increased from 45.65% in the flood season to 46.00% in the non-flood season.

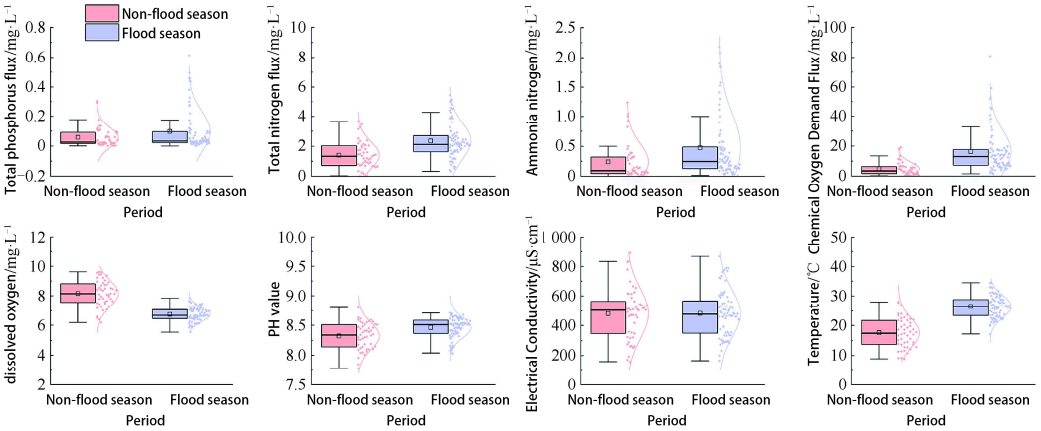


Figure 2. Comparison of the river water quality indexes between the flood and non-flood seasons in the Xiaojiang River Basin. Note that: Distribution of water quality indicators across seasons/zones using a box–violin plot. The box represents the interquartile range (IQR; 25th–75th percentiles), and the horizontal line inside the box indicates the median. The whiskers extend to the minimum and maximum values within 1.5 × IQR. The square marker inside the box denotes the mean. Individual observations are shown as jittered points, and the half-violin on the right depicts the kernel density distribution, illustrating the overall data distribution.

3.1.2. Spatial Distribution of Water Quality Indicators

As shown in Figure 3 and Table 3, the average water quality index values differ between the flood and non-flood seasons across the three zones. In residential areas, total phosphorus, total nitrogen, ammonia nitrogen, COD, conductivity, and temperature were higher during the flood season than the non-flood season, while dissolved oxygen showed the opposite trend. In the cultivated land areas, the total nitrogen, ammonia nitrogen, COD, electrical conductivity, and temperature were higher in the flood season than in the non-flood season. The opposite was true for dissolved oxygen, while the total phosphorus and pH values were the same. In hazard-prone areas, all indicators except dissolved oxygen showed higher values during the flood season than during the non-flood season. The average values of total phosphorus, total nitrogen, ammonia nitrogen, COD, and conductivity generally followed the trend of hazard-prone areas > residential areas > cultivated land areas, while the dissolved oxygen and pH indicators showed a trend of cultivated land areas > residential areas > hazard-prone areas.

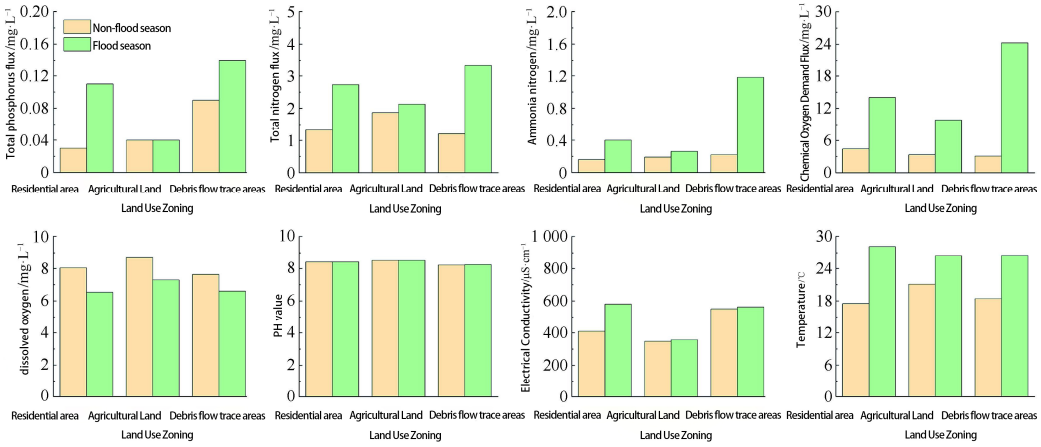


Figure 3. The average water quality of different land-use zones in Xiaojiang River Basin.

Table 3. Comparison of the main water quality indexes in the three regions of the Xiaojiang River Basin.

	Residential Area		Cultivated Land Area		Hazard-Prone Area	
	Non-Flood Season	**Flood Season**	**Non-Flood Season**	**Flood Season**	**Non-Flood Season**	**Flood Season**
Total phosphorus (mg/L)	0.03	0.11	0.04	0.04	0.09	0.14
Total nitrogen (mg/L)	1.32	2.73	1.87	2.13	1.20	3.35
Ammonia nitrogen (mg/L)	0.16	0.40	0.19	0.26	0.22	1.18
COD (mg/L)	4.42	14.04	3.35	9.84	3.09	24.27
Dissolved oxygen (mg/L)	8.04	6.53	8.67	7.29	7.63	6.60
Conductivity (μs/cm)	409.85	581.21	348.11	357.17	551.19	562.83
pH	8.41	8.41	8.50	8.50	8.22	8.24
Temperature (°C)	17.52	28.14	21.10	26.48	18.41	26.52

In Figure 4, non-flood season water quality indicators are represented by semi-transparent red-orange circles of varying sizes, while flood season indicators are depicted by opaque green circles of varying sizes. Water quality indicators show no significant difference between flood and non-flood seasons.

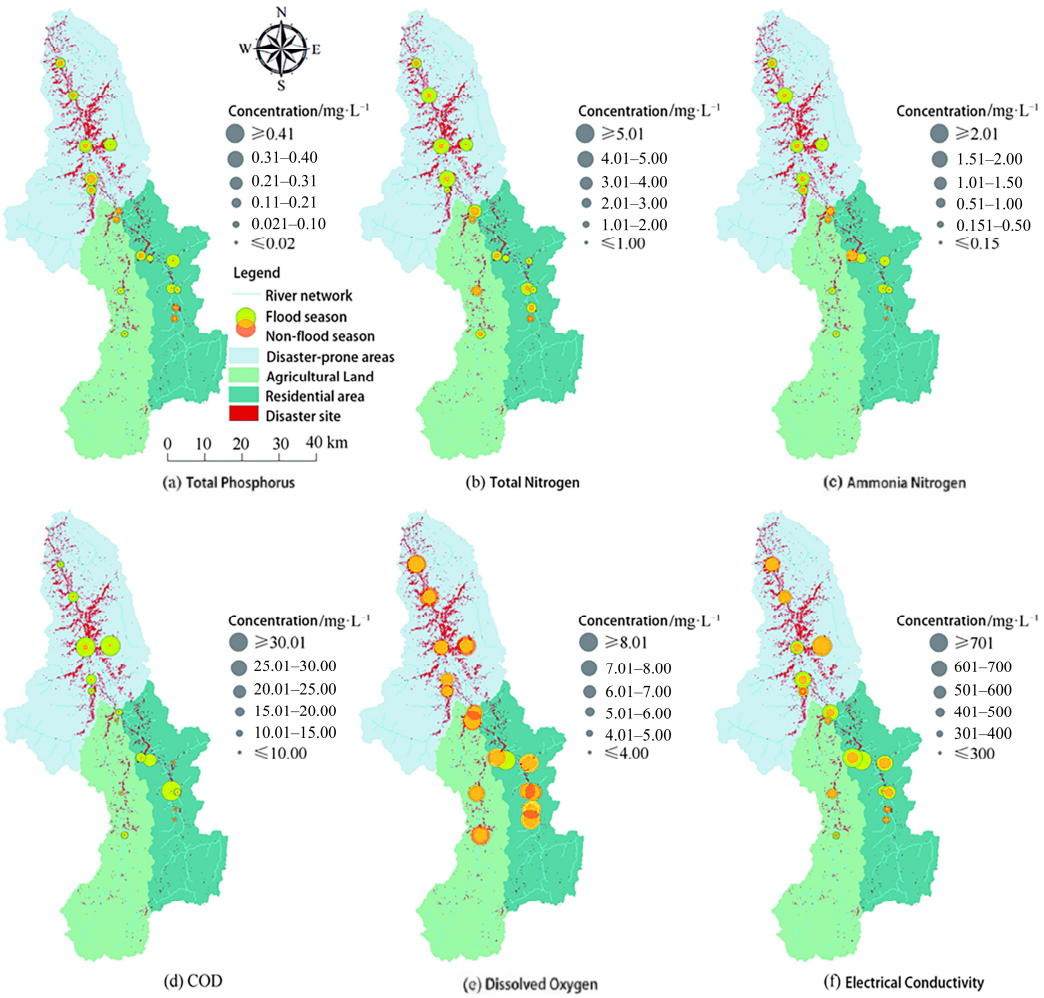


Figure 4. Spatial distribution of river water quality indexes in the Xiaojiang River Basin.

Significant variations exist in typical water quality indicator concentrations and water quality conditions across different land-use zones. The concentration ranges of indicators such as total phosphorus, total nitrogen, ammonia nitrogen, and COD show a trend of "hazard-prone areas > residential areas > cultivated land areas", while the concentration

ranges of dissolved oxygen and electrical conductivity have relatively small differences. Taking total nitrogen and COD as examples, the concentration ranges in cultivated land areas were 1.19–2.52 mg/L and 1.00–12.25 mg/L, respectively. The concentration ranges range in residential areas were 0.48–3.79 mg/L and 2.70–34.39 mg/L, respectively. The concentration range in the debris flow trace areas was the largest, ranging from 0.11 to 4.37 mg/L and 1.15 to 49.21 mg/L, respectively. The average concentrations of total phosphorus, total nitrogen, ammonia nitrogen, COD, and conductivity also followed the trend "hazard-prone areas > residential areas > cultivated land areas", while dissolved oxygen showed the opposite pattern. For instance, the average concentrations of total nitrogen and COD in the hazard-prone areas were 2.28 mg/L and 27.36 mg/L, respectively, which were significantly higher than 2.03 mg/L and 9.23 mg/L in residential areas, as well as 2.00 mg/L and 6.60 mg/L in cultivated land areas. It further reveals the differential influence of land-use types on water pollution load.

From the perspective of flow direction in the Xiaojiang River Basin, the concentrations of indicators such as total phosphorus, total nitrogen, ammonia nitrogen, and COD generally show a gradient distribution with lower concentrations in the upper reaches and higher concentrations in the lower reaches. Dissolved oxygen, however, shows the opposite trend, while conductivity does not exhibit significant flow-direction characteristics. Taking total phosphorus and ammonia nitrogen as examples, in the upstream residential and cultivated land areas, there were three sampling points with total phosphorus concentrations exceeding 0.10 mg/L, while in the downstream debris flow trace areas, this number increased to eight. Similarly, sampling points with ammonia nitrogen concentrations exceeding 0.50 mg/L numbered 5 and 8, respectively, indicating a more pronounced cumulative effect of pollutants in the downstream areas.

The water quality analysis of the branch gullies shows that the pollution levels of different branch gullies vary significantly owing to the distribution differences in the debris flow trace areas. For example, Anni Gully, unaffected by hazard area, maintained stable levels of total phosphorus, total nitrogen, ammonia nitrogen, COD, and conductivity during both flood and non-flood seasons. Jiangjia Gully, with a densely distributed hazard area, exhibited significantly elevated water quality indicators (except conductivity) during the flood season. Specifically, Jiangjia Gully's total phosphorus concentration was 0.01 mg/L during the non-flood season but increased to 0.236 mg/L during the flood season. Ammonia nitrogen concentration rose from 0.02 mg/L to 1.44 mg/L. This indicates that the hazard area has a critical impact on water quality deterioration during the flood season.

3.2. Influencing Factors of Water Quality Changes

3.2.1. Changes in Key Water Quality Indicators Before and After Heavy Rainfall Events

Figure 5 illustrates the changes in key water quality fluxes before and after the event-based heavy rainfall in the Xiaojiang River Basin. Considering the timeliness of the rainfall event, this study selected only seven sampling points within the Xiaojiang River Basin for monitoring, covering two main stream sampling points in residential areas (D2, D3), one main stream sampling point in cultivated land areas (K3), three main stream sampling points in debris flow trace areas (X1, X3, X4), and one typical branch gully sampling point located in a debris flow trace areas (JG). Monitoring results indicate that rainfall events significantly impact watershed water quality, particularly during the short period following heavy rainfall, when pollutant transport in water bodies increases markedly.

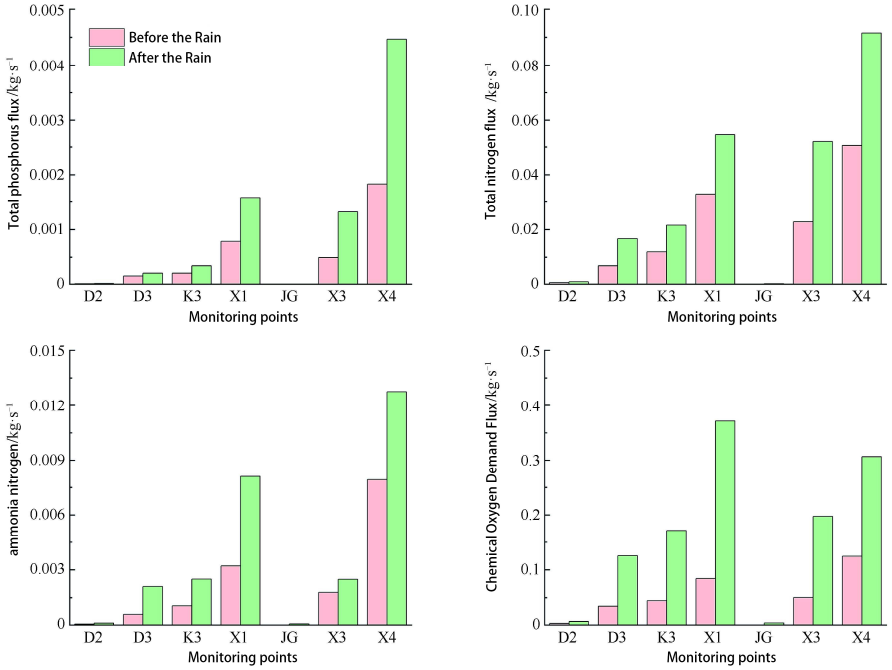


Figure 5. Comparison of the fluxes of main pollutants in the main stream before and after heavy rainfall events.

Before the rainstorm occurred, the total phosphorus flux in the main stream of residential areas was the smallest, being 8.00×10^{-6} kg/s and 1.50×10^{-5} kg/s, respectively. The cultivated land areas exhibited slightly higher fluxes at 1.96×10^{-4} kg/s, while the debris flow trace areas showed the highest fluxes of 7.87×10^{-4} kg/s, 4.96×10^{-4} kg/s, and 1.83×10^{-3} kg/s. The total nitrogen, ammonia nitrogen, and COD fluxes exhibited similar trends, generally presenting as "hazard-prone areas > cultivated land areas > residential areas". Following the heavy rainfall, key water quality fluxes at all sampling sites increased significantly. Total phosphorus flux in the residential area's main stream rose to 1.30×10^{-5} kg/s and 2.00×10^{-5} kg/s, respectively, while the flux in the cultivated land area increased to 3.47×10^{-4} kg/s, and the fluxes in the hazard-prone area increased to 1.58×10^{-3} kg/s, 1.32×10^{-3} kg/s, and 4.47×10^{-3} kg/s, respectively. Overall, the fluxes of key water qualities generally showed a geometric multiple increase after heavy rain. The average growth rates of total phosphorus, total nitrogen, ammonia nitrogen and COD were 1.95, 2.41, 2.34 and 4.74 times, respectively. Among them, the COD flux at sampling point X1 in the hazard-prone area had the largest growth rate, with an increase of 5.13 times. The smallest increase was observed in the total phosphorus flux at sampling point D2 in the residential area, which increased by 1.35 times.

Jiangjia Gully, as a typical branch gully with frequent geological disasters, has a debris flow trace area that accounts for 21.77% of the sub-basin area. Following heavy rainfall events, the key water quality indicators of Jiangjiagou performed particularly outstandingly, especially the growth rate of COD flux which reached 12.58 times, significantly higher than the maximum growth rate in the main stream area. Concurrently, the average growth rate across the four key water quality indicators reached 6.41-fold, surpassing the mainstem's maximum growth rate by 1.28-fold.

3.2.2. Impact of Landscape Pattern on Water Quality

To further investigate the impact of the debris flow trace area on water quality, this study employed seven landscape pattern indices across different land-use types as explanatory variables. Two typical scales (1000 m river buffer zone scale and sub-basin scale) were selected, and water quality indices were used as response variables for redundancy analysis

(RDA). The results of the redundancy analysis are presented in Figure 6 and Table 4, with landscape pattern indices for each "category" denoted as "Landscape Pattern Index land use Type". Table 4 reveals the seasonal and spatial differences in the impact of landscape patterns on water quality. The selected landscape indicators explained over 94.00% of water quality variation during the flood season, while the total explained volume decreased by 5.66–5.85% during the non-flood season. The first principal component (axis) of the river buffer zone contributed the most as an explanatory variable during the flood season, at 59.83%, while it was relatively smaller during the non-flood season. By comparing the explanatory power of water quality in different periods, the role of landscape patterns in the dynamic changes in water quality in different periods can be further understood. The spatial distribution of disaster-stricken areas, forest land, and cultivated land within the river buffer zone during the flood season. The model determines significant changes in water quality indicators, especially in key water qualities such as total phosphorus, ammonia nitrogen, and COD flux.

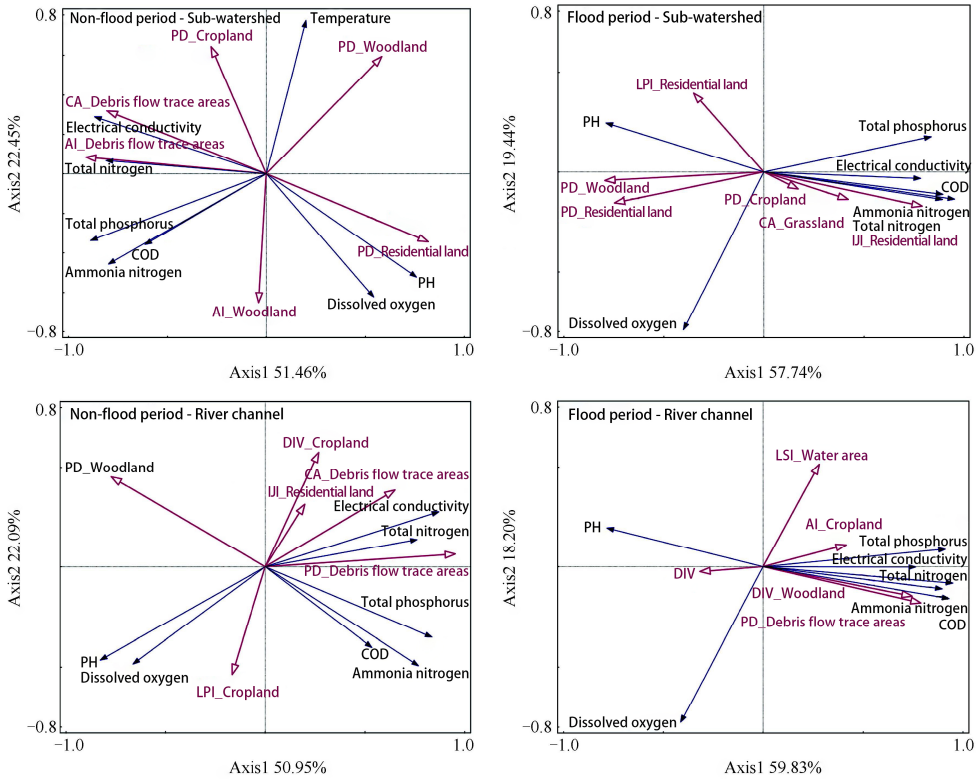


Figure 6. Multivariate analysis diagram of landscape pattern indexes and river water quality indexes based on redundancy analysis.

Table 4. The explanation rates of landscape pattern indexes to the river water quality variations.

Scale	Period	Explanatory Variables (%)				Complete Explanatory Variable (%)	Contribution of Key Landscape Pattern Index (%)
		Axis 1	Axis 2	Axis 3	Axis 4		
Sub-basin	non-flood season	51.46	22.45	10.77	6.17	90.84	AI_hazard-influenced area (43.1), AI-forest land (15.5)
	flood season	57.74	19.44	8.56	5.92	96.50	IJI-residential area (40.7), PD-forest land (17.7)
River course	non-flood season	50.95	22.09	9.17	5.97	88.15	PD_hazard-influenced area (46.8), PD-forest land (15.3)
	flood season	59.83	18.20	9.97	6.00	94.00	PD_hazard-influenced area (40.1), DIV-cultivated land area (16.8)

Figure 6 illustrates the multivariate analysis between landscape pattern indices and water quality indicators. Red arrows represent landscape pattern indices, while blue arrows denote water quality indices. An angle between the two indices less than 90° indicates a positive correlation, whereas a larger angle suggests a negative correlation. A longer projection length from one index to another indicates a stronger correlation.

At the sub-basin scale, the most significant explanatory variable during the non-flood season was AI_hazard-influenced areas, which explained 43.10% of the water quality changes. Increased AI_hazard-influenced areas showed a highly significant positive correlation with total nitrogen and significant positive correlations with total phosphorus, ammonia nitrogen, COD flux, and conductivity. This indicates that the higher the concentration of hazard area, the more significant the changes in pollutant levels and water quality. Specifically, the distribution characteristics of hazard area directly determine the transport and accumulation of key pollutants in water bodies, particularly during the non-flood season when landscape pattern changes may lead to more pronounced water pollution. During the flood season, the most significant explanatory variable was IJI-residential land-use, contributing 40.70% to the explanation of water quality, demonstrating the sensitivity of water quality changes to the spatial distribution of residential areas. As the spatial adjacency of residential land patches with other land-use types diversifies and their distribution expands, the magnitude of water quality changes increases accordingly. This effect was particularly pronounced for total phosphorus, total nitrogen, ammonia nitrogen, COD flux, and electrical conductivity, reflecting the interaction between flood-induced water scouring and residential distribution patterns during the flood season, where residential expansion and uneven distribution further exacerbate pollutant migration and accumulation.

At the river scale, the landscape pattern index with the greatest contribution during the non-flood season was PD_hazard-influenced areas, with a contribution rate of 46.8%. PD_hazard-influenced areas showed significant positive correlations with total nitrogen flux and conductivity, and positive correlations with total phosphorus, ammonia nitrogen, and COD flux. This indicates that a higher number of the debris flow trace area per unit area leads to more pronounced changes in pollutant concentrations and water quality. This finding further substantiates the role of the debris flow trace area as sources of water pollution, particularly across different parts of the watershed, and holds significant implications for water quality management and pollution control. Analysis results during the flood season were similar to those outside the flood season, with PD_hazard area remaining the most influential landscape pattern index, contributing 40.1%. During this period, the distribution of disaster sites exerted a more pronounced impact on water quality, notably exhibiting increased positive correlations with total phosphorus, ammonia nitrogen, and COD fluxes. This indicates that enhanced water flow during the flood season intensified pollutant inputs from disaster sites. Additionally, the landscape separation index for cultivated land (DIV_cultivated land) emerged as the second most influential factor in water quality variation, indicating that more dispersed cultivated land correlates with lower key water quality flux values. The dispersion of cultivated land partially mitigates water quality deterioration, particularly during the flood season, when rational land distribution effectively reduces pollutant transport and dispersion.

4. Discussion

4.1. Attribution of Temporal and Spatial Distribution Differences in Water Quality in River Basins

Differences in rainfall are the key factors causing variations in water quality between the flood and non-flood seasons in the Xiaojiang River Basin. The phenomenon of poorer water quality during the flood season compared to the non-flood season is primarily related to factors such as precipitation, runoff intensity, topography, landform [47], and pollutant

input pathways [48]. Intense precipitation events rapidly wash pollutants from soil into water bodies, particularly agricultural and urban non-point source pollution, which enter water bodies in large quantities via runoff [49]. Rainfall during the flood season accounts for 85% [50] of the annual precipitation in the Xiaojiang River Basin. As a mountainous river, the Xiaojiang River Basin is not only a region with strong human activity but also one where geological disasters occur frequently. This area not only faces the problems of agricultural non-point source pollution and urban non-point source pollution, but also, owing to its mountainous terrain and steep slopes, is strongly affected by geological disasters such as soil erosion, resulting in significant differences in key water quality concentrations between the flood and non-flood seasons. The research of Sihe Deng et al. [51] pointed out that the seasonal variation in water quality is mainly driven by human social and economic activities and land-use types. The study by Siru Wang et al. [38] further indicated that the total nitrogen and total phosphorus loads during the flood season accounted for 65.0% and 63.2% of the annual total load, respectively. The variations in these loads are closely related to factors such as annual runoff depth and geological disasters. Therefore, water quality management strategies must fully consider seasonal differences, especially during the flood season, and adopt targeted control measures. Specifically, measures should be taken to control urban runoff to ensure it meets national discharge standards, and ecological construction (such as terraced field construction) and conservation tillage (such as no-till farming) should be strengthened. Precise fertilization can effectively reduce the loss of nutrients in farmland, while scientific management of hazard area and reduction in soil erosion are important links to reduce the input of pollutants during the flood season [52]. These measures can help slow down the rate of water quality deterioration and protect the health of aquatic ecosystems.

Water quality exhibits temporal variability and significant spatial differences. Research indicates that water quality concentrations in downstream hazard-prone areas are significantly higher than in upstream residential and cultivated land areas, with residential areas showing higher concentrations than cultivated land areas. The research conducted by Ting Zhou et al. [53] in the Dongjiang River Basin pointed out that due to the accumulation and propagation effects of pollutants, the water quality concentration in the lower reaches was significantly higher than that in the upper reaches. Furthermore, other studies indicate that disasters trigger massive releases of organic matter, leading to long-term changes in aquatic communities (lasting 32 years) [31], which in turn alter water quality concentrations. In particular, during the flood season, heavy rainfall and continuous downpours usually intensify the inflow of sediment in disaster-stricken areas, and the content of particulate matter in water bodies is a key factor affecting water quality [54,55].

Beyond physical transport processes (e.g., hillslope erosion), biogeochemical processes during the flood season also interact with runoff-driven wash-off, suspended sediment transport, and mixing/dilution, thereby shaping the temporal dynamics of water quality [56]. Intense rainfall and flood events often deliver large amounts of fine suspended sediments and particulate organic matter, increasing turbidity, limiting light penetration, and suppressing primary production, which in turn reduces in-stream oxygen production [57]. Moreover, in mountainous river basins with pronounced contrasts between flood and non-flood seasons, such as the Xiaojiang River Basin, dried and exposed streambeds can become biogeochemically active hotspots: accumulated substrates, a high abundance of nitrogen-transformation genes, and favorable moisture conditions can promote denitrification [58]. The fact that NH_3-N shows the largest seasonal change rate in Table 3 may also be linked to these processes. Rainfall-induced rewetting can further stimulate microbial activity in dried streambeds, including oxygen-consuming microbial processes, thereby

increasing oxygen demand and lowering dissolved oxygen (DO) during the flood season, which is consistent with previous findings [58–60].

4.2. Impact of the Debris Flow Trace Area on River Water Quality in the Xiaojiang Basin

To investigate the relationship between key water quality parameters and disaster-affected areas, this study quantified sediment transport rates and hazard area sizes during flood and non-flood seasons for three primary tributaries of the Xiaojiang River: Annie Gully, Taojia Small River, and Jiangjia Gully. Annie Gully has not experienced debris flow disasters for many years, with its debris flow trace areas constituting 0.12% of the total area. Taojia Small River was once an area frequently affected by landslides and debris flows. In recent years, through natural restoration and human governance, the number of such disasters has gradually decreased. The area affected by these disasters now accounts for 1.23% of the total area. Jiangjiagou is an area where landslides and debris flows occur frequently and is known as the "Natural Museum of Debris Flows". The area affected by the disaster accounted for 21.77% of the total area (Figure 7). During the non-flood season, Jiangjia Gully had the lowest sediment transport rate, followed by Taojia Small River and Annie Gully. During the flood season, the sediment transport rates of Annie Gully, Taojia Small River, and Jiangjia Gully were 0.42 kg/s, 2.14 kg/s and 7.33 kg/s, respectively. Among them, Jiangjia Gully had the largest increase, reaching 733,100.00%. It can be observed that as the proportion of the hazard area increases, the sediment transport rate of the branch gullies increases significantly (Table 5).

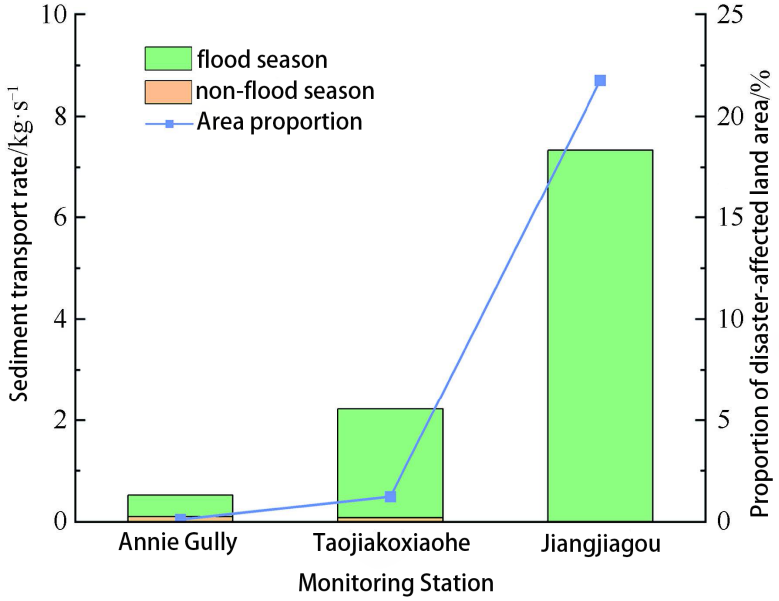


Figure 7. Sediment transport rate of branch ditch and proportion of disaster area.

Table 5. Sediment discharges and area proportion of hazard-influenced areas in the three typical gullies.

Location	Sand Transport Rate of Non-Flood Season (kg/s)	Sand Transport Rate of Flood Season (kg/s)	Proportion of Hazard Area (%)
Anni Gully	0.105	0.417	0.118
Taojia Small River	0.080	2.141	1.229
Jiangjia Gully	0.001	7.332	21.765

Subsequently, we conducted a week-long sediment-water quality monitoring campaign on the main stream of the Xiaojiang River Basin, and the results revealed a positive

correlation between key water quality fluxes and sediment transport flux (Figure 8). Among these, total phosphorus flux exhibited the best fit with sediment transport flux, with an R^2 value of 0.67, whereas COD flux showed the poorest fit with sediment transport flux (R^2 = 0.33). In conclusion, key water quality fluxes vary with sediment transport flux and exhibit strong correlation. Liu Rui's research indicates that the increase in particulate matter in rivers during the flood season has a significant impact on the phosphorus content in the Wei River water, exceeding the changes brought about by total organic matter and total nitrogen [54]. Research in the lower reaches of the Jinsha River also found that the total nitrogen concentration changed little with the sediment content, while the total phosphorus concentration was positively correlated with the sediment content [61]. Ultimately, we confirmed that the disaster site led to an increase in river sediment transport, thereby significantly affecting the flux of key water quality parameters. In the future, in the water environment governance of multiple hazard areas, we should strengthen the management of areas frequently affected by debris flows (such as Jiangjia Gully), implement scientific measures for the restoration of hazard areas, and reduce the inflow of sediment into water bodies from hazard areas. The stability of restored areas, such as Anni Gully, should be continuously monitored to prevent the recurrence of disasters.

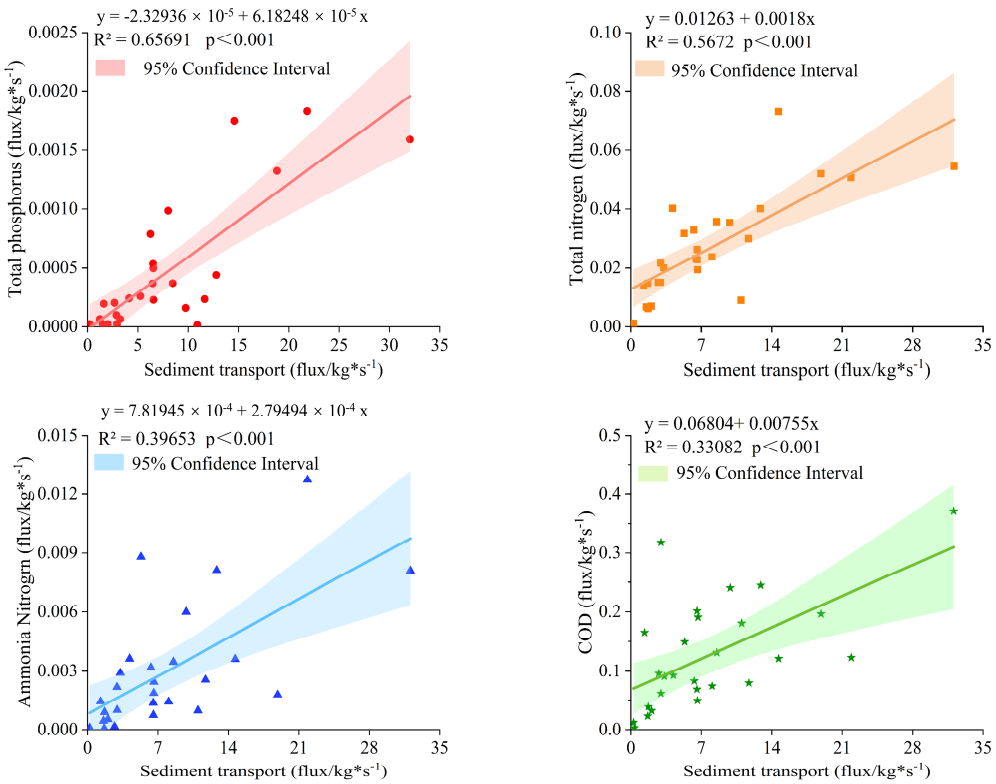


Figure 8. Relationships of sediment and the fluxes of main pollutants in the Xiaojiang River Basin.

4.3. Impact of Landscape Pattern Characteristics in the Xiaojiang River Basin on River Water Quality

The spatial configuration of landscapes plays a crucial role in determining ecological processes, such as nutrient cycling, hydrological processes, and energy flow [62]. Landscape pattern characteristics, including size, density, aggregation, and diversity, are key land-use features that influence river water quality [21]. In this study, the AI_hazard area, PD_hazard area, and IJI_residential area all showed positive correlations with key water quality indicators, ranking as the most influential landscape pattern indices among the four buffer zones. The more concentrated the non-flood season hazard area at the sub-basin scale (the larger the AI_hazard area index), the greater the total nitrogen index, whereas the larger the AI of the forest land, the lower the total nitrogen index. Shehab et al.'s [29]

research in Malaysia also shows that if forests are not dispersed, water quality may be better. Forests and grasslands sequester and absorb pollutants within river systems. Furthermore, forest cover acts as a filter or sieve, trapping and reducing pollutants and sediments carried by surface runoff [63]. At the sub-basin scale during the flood season, the IJI-residential area showed a positive correlation with key water quality indicators and was the most influential factor explaining water quality. Residential areas are well-known contributors to water quality degradation [64], exerting exceptionally strong and significant impacts on water quality, even when urban areas constitute a relatively small proportion [53]. At the river channel scale, the PD_hazard area contributed most significantly to water quality interpretation during both flood and non-flood seasons. This index also showed strong correlations with key water quality indicators, including total phosphorus, total nitrogen, ammonia nitrogen, and COD, indicating that at the river scale, higher fragmentation of the debris flow trace areas leads to poorer river water quality. Conversely, the PD_forest index was negatively correlated with key water quality indicators; therefore, future management efforts in hazard-prone areas should prioritize the protection of forests and grasslands, particularly in the upstream and high-risk regions of watersheds, as forest connectivity and continuity play a crucial role in water quality protection. Strengthening forest conservation and expanding vegetation cover can reduce soil erosion and pollutant input into water bodies.

4.4. Implications and Limitations

Under the combined pressures of climate change, intensive human activities, and frequent geological hazards, our results show that water quality deterioration in dry-hot valley basins is strongly season- and event-dependent, with the flood season exhibiting higher concentrations/loads of key pollutants (TN, TP, NH_3-N, and COD) than the non-flood season. The consistent spatial gradient (hazard-prone area > residential area > cultivated land area) suggests that management should prioritize flood-season runoff control and targeted mitigation in downstream hazard-prone areas and debris-flow-affected tributaries while leveraging landscape-based interventions (e.g., reducing PD_hazard-influenced areas and optimizing IJI_residential areas) alongside soil and water conservation and ecological restoration to support watershed management in Southwest China and the Baihetan Reservoir area.

Our conclusions are based on observational monitoring and mainly reflect associations rather than strict causality; given the lack of higher-frequency, cross-scale, and well-replicated site–event time series with synchronized covariates, we did not implement PLM-SEM/SEM or Granger causality analysis to test direct/indirect pathways and lagged directional effects [65]. In addition, intermittent low flows in some branch gullies and the absence of continuous stage–discharge records limit year-round quantification of tributary flow fractions and load contributions [66]. Finally, we relied on conventional physicochemical indicators, and thus source attribution remains uncertain; future work should incorporate stable isotopes or source-tracing indicators (e.g., $\delta^{15}N$–NO_3^-, $\delta^{18}O$–NO_3^-) together with dissolved-particulate partitioning [67,68]. These gaps can be addressed through continuous hydro–water quality monitoring and coupled watershed modeling (e.g., a calibrated SWAT hydrology–water quality model), which would also provide the data basis for PLM-SEM/SEM and Granger-based analyses [69–71].

5. Conclusions

This study conducted a systematic quantitative study on the influence of the dry-hot valley basin landscape pattern of “severe anthropogenic activities and frequent geolog-

ical hazards" in the lower reaches of the Jinsha River on the spatio-temporal variation characteristics of river water quality. The main conclusions are as follows:

(1) The key water quality indices, such as total phosphorus, total nitrogen, ammonia nitrogen, chemical oxygen demand, and temperature in the Xiaojiang River Basin were shown as flood season > non-flood season. During the non-flood season, the dissolved oxygen and conductivity indicators showed a trend of being greater than those during the flood season, whereas the pH value remained unchanged. The data for total phosphorus, total nitrogen, ammonia nitrogen, and COD indicators had a relatively large degree of dispersion during the flood and non-flood seasons, whereas dissolved oxygen and pH values showed the opposite trend.

(2) From a spatial perspective, the water quality in each land-use zone during the non-flood season was better than that during the flood season. The average concentrations, concentration ranges, and water quality conditions of total phosphorus, total nitrogen, ammonia nitrogen, COD, and electrical conductivity were in the following order: hazard-prone area > residential area > cultivated land area. In addition, the water quality in the upstream was generally better than that in the downstream. The larger the proportion of disaster-affected sites in the branch gullies, the more severe the deterioration of water quality during the flooding season.

(3) Under heavy rain conditions in each session, the transport volume of nitrogen and phosphorus pollutants in water bodies increased significantly. In the branch gully areas with a large proportion of disaster-stricken areas and debris flow trace areas, the pollutant fluxes increased geometrically.

(4) The results of redundancy analysis (RDA) showed that the ability of landscape patterns in the flood season to explain the change in water quality was better than that in the non-flood season. At the sub-basin scale, the higher the aggregation degree of non-flood season disaster sites (AI_ hazard-influenced areas), the higher the concentrations of nitrogen, phosphorus, and organic pollutants in key water quality indicators, and the greater the risk of water quality deterioration. The distribution of residential land during the flood season and the increase in the adjacency index (IJI_ residential area) were positively correlated with the variation range of water quality, indicating that the diversity of contact between residential land and other patch types aggravated water pollution. At the river channel scale, the degree of fragmentation of the disaster site (PD_hazard-influenced areas) significantly exacerbated the pollution level. The degree of landscape dispersion of cultivated land (DIV_cultivated land) effectively reduces water pollution, especially having a significant inhibitory effect on the increase in key water quality indicators such as total phosphorus and total nitrogen in main and tributary streams.

Author Contributions: H.T.: Writing—original draft, Methodology, Conceptualization. J.Y.: Methodology, Formal analysis. C.Y.: Writing—review and editing. S.L.: Formal analysis. L.Q.: Formal analysis. L.Z.: Formal analysis. C.T.: Methodology. H.R.: Supervision. Y.Y.: Supervision. All authors have read and agreed to the published version of the manuscript.

Funding: This research was funded by the National Natural Science Foundation of China grant number 52469014, and by the Young Talent Project of the "Xingdian Talent Support Program" of Yunnan Province (2022). APC: This research was funded by [the National Natural Science Foundation of China] grant number [52469014]. And The APC was funded by [the National Natural Science Foundation of China] grant number [52469014].

Data Availability Statement: The original contributions presented in the study are included in the article material. Further inquiries can be directed to the corresponding author.

Acknowledgments: This research was financially supported by the National Natural Science Foundation of China (Grant No. 52469014), the Young Talent Project of the "XingdianTalent Support Program of Yunnan Province in 2022.

Conflicts of Interest: Authors Chunyu Yang, Songpei Li, and Liang Qi were employed by th ecompany Huadian Jinsha River Midstream Hydropower Development Co., Ltd., Kunming, Yunnan, China. The remaining authors declare that the research was conducted in the absence of any commercial or financial relationships that could be construed as a potential conflict of interest.

References

1. Zhang, J.; Liu, C.; Xu, J. Earth Critical Zone: A comprehensive exploration of the Earth's surface processes. *Earth Crit. Zone* **2024**, *1*, 100001. [CrossRef]
2. Allan, J.D. Landscapes and riverscapes: The influence of land use on stream ecosystems. *Annu. Rev. Ecol. Evol. Syst.* **2004**, *35*, 257–284. [CrossRef]
3. Tiwari, A.K.; Suozzi, E.; Silva, C.; De Maio, M.; Zanetti, M. Role of Integrated Approaches in Water Resources Management: Antofagasta Region, Chile. *Sustainability* **2021**, *13*, 1297. [CrossRef]
4. Naylor, L.A.; Dungait, J.A.J.; Zheng, Y.; Buckerfield, S.; Green, S.M.; Oliver, D.M.; Liu, H.; Peng, J.; Tu, C.; Zhang, G.-l.; et al. Achieving Sustainable Earth Futures in the Anthropocene by Including Local Communities in Critical Zone Science. *Earths Future* **2023**, *11*, e2022EF003448. [CrossRef]
5. Zhai, X.; Xia, J.; Zhang, Y. Water quality variation in the highly disturbed Huai River Basin, China from 1994 to 2005 by multi-statistical analyses. *Sci. Total Environ.* **2014**, *496*, 594–606. [CrossRef]
6. Yue, F.-J.; Waldron, S.; Li, S.-L.; Wang, Z.-J.; Zeng, J.; Xu, S.; Zhang, Z.-C.; Oliver, D.M. Land use interacts with changes in catchment hydrology to generate chronic nitrate pollution in karst waters and strong seasonality in excess nitrate export. *Sci. Total Environ.* **2019**, *696*, 134062. [CrossRef]
7. Wang, W.; Liu, C.; Zhang, F.; Tan, M.L.; Shi, J.; Zhang, Z.; Duan, P.; Kung, H.-T.; Xin, H. Evaluation of impacts of environmental factors and land use on seasonal surface water quality in arid and humid regions using structural equation models. *Ecol. Indic.* **2022**, *144*, 109546. [CrossRef]
8. Van Vliet, M.T.H.; Thorslund, J.; Strokal, M.; Hofstra, N.; Floerke, M.; Macedo, H.E.; Nkwasa, A.; Tang, T.; Kaushal, S.S.; Kumar, R.; et al. Global river water quality under climate change and hydroclimatic extremes. *Nat. Rev. Earth Environ.* **2023**, *4*, 687–702. [CrossRef]
9. Dethier, E.N.; Renshaw, C.E.; Magilligan, F.J. Rapid changes to global river suspended sediment flux by humans. *Science* **2022**, *376*, 1447–1452. [CrossRef]
10. Xiang, X.; Wang, W.; Wu, X.; Liu, Z.; Rajib, A.; Wu, L.; Cao, H.; Lin, X.; Liu, Y. Effects of Deep Learning Bias Correction and Carbon Neutrality on Projections of Future Population Exposure to Extreme Precipitation. *Int. J. Climatol.* **2026**, *46*, e70174. [CrossRef]
11. Wang, M.; Bodirsky, B.L.; Rijneveld, R.; Beier, F.; Bak, M.P.; Batool, M.; Droppers, B.; Popp, A.; van Vliet, M.T.H.; Strokal, M. A triple increase in global river basins with water scarcity due to future pollution. *Nat. Commun.* **2024**, *15*, 880. [CrossRef] [PubMed]
12. Deng, X. Influence of water body area on water quality in the southern Jiangsu Plain, eastern China. *J. Clean. Prod.* **2020**, *254*, 120136. [CrossRef]
13. Bridgewater, P.; Upadhaya, S.; Poudyal, B. Understanding and managing inland water biodiversity in the earth critical zone. *Earth Crit. Zone* **2025**, *2*, 100023. [CrossRef]
14. Battin, T.J.; Lauerwald, R.; Bernhardt, E.S.; Bertuzzo, E.; Gener, L.G.; Hall, R., Jr.; Hotchkiss, E.R.; Maavara, T.; Pavelsky, T.M.; Ran, L.S.; et al. River ecosystem metabolism and carbon biogeochemistry in a changing world. *Nature* **2023**, *613*, 449–459. [CrossRef]
15. Agyekum, M.K.; Pathak, D.; Kindinger, A.; Kumar, R.; Borchardt, D.; Weitere, M.; Frank, K.; Schmitt-Jansen, M.; Büttner, O.; Brauns, M.; et al. A hydrologically informed agricultural land use intensity index for assessing ecological impacts on streams and rivers. *Commun. Earth Environ.* **2025**, *6*, 991. [CrossRef]
16. Baccour, S.; Goelema, G.; Kahil, T.; Albiac, J.; van Vliet, M.T.H.; Zhu, X.; Strokal, M. Water quality management could halve future water scarcity cost-effectively in the Pearl River Basin. *Nat. Commun.* **2024**, *15*, 5669. [CrossRef]
17. Puczko, K.; Jekatierynczuk-Rudczyk, E. Extreme Hydro-Meteorological Events Influence to Water Quality of Small Rivers in Urban Area: A Case Study in Northeast Poland. *Sci. Rep.* **2020**, *10*, 10255. [CrossRef]
18. Zhong, X.C.; Xu, Q.L.; Yi, J.H.; Jin, L.J. Study on the threshold relationship between landscape pattern and water quality considering spatial scale effect—A case study of Dianchi Lake Basin in China. *Environ. Sci. Pollut. Res.* **2022**, *29*, 44103–44118. [CrossRef]

19. Zheng, Y.X.; Li, C.; Yu, J.S.; Wang, Q.Y.; Yue, Q.M. Tracking the optimal watershed landscape pattern for driving pollutant transport: Insights from the integration of mechanistic models and data-driven approaches. *J. Environ. Manag.* **2025**, *37*, 123939. [CrossRef]
20. Li, S.K.; Tu, B.; Zhang, Z.; Wang, L.; Zhang, Z.; Che, X.Q.; Wang, Z.Z. Exploring new methods for assessing landscape ecological risk in key basin. *J. Clean. Prod.* **2024**, *461*, 142633. [CrossRef]
21. Lee, S.W.; Hwang, S.J.; Lee, S.B.; Hwang, H.S.; Sung, H.C. Landscape ecological approach to the relationships of land use patterns in watersheds to water quality characteristics. *Landsc. Urban Plan.* **2009**, *92*, 80–89. [CrossRef]
22. Alberti, M.; Booth, D.; Hill, K.; Coburn, B.; Avolio, C.; Coe, S.; Spirandelli, D. The impact of urban patterns on aquatic ecosystems: An empirical analysis in Puget lowland sub-basins. *Landsc. Urban Plan.* **2007**, *80*, 345–361. [CrossRef]
23. Zhang, M.S.; Li, W.; Zhang, W.G.; Li, Y.T.; Li, J.Y.; Gao, Y. Agricultural land-use change exacerbates the dissemination of antibiotic resistance genes via surface runoffs in Lake Tai Basin, China. *Ecotoxicol. Environ. Saf.* **2021**, *220*, 112328. [CrossRef] [PubMed]
24. Huang, L.; Chen, Q.J.; Feng, J.Z. Spatial-temporal characteristics and driving mechanisms analysis of habitat quality in Shenfu mining area based on geodetector. *Solid. Earth* **2023**, *39*, 451–463. [CrossRef]
25. Wang, Z.; Johnson, D.A.; Rong, Y.; Wang, K. Grazing effects on soil characteristics and vegetation of grassland in northern China. *Solid Earth* **2016**, *7*, 55–65. [CrossRef]
26. He, L.J.; Huang, L.B.; Ke, X.L. The analysis of the impact of slope climbing of cultivated cand on ecosystem services in the Yangtze River Basin. *Acta Ecol. Sin.* **2025**, *45*, 367–384. [CrossRef]
27. Yang, L.Y.; Chen, W.X.; Zeng, J. Gradient differences of the impact of urbanization on habitat quality in the Yangtze River Basin. *Acta Ecol. Sin.* **2024**, *44*, 4038–4050. [CrossRef]
28. Shehab, Z.N.; Jamil, N.R.; Aris, A.Z.; Shafie, N.S. Spatial variation impact of landscape patterns and land use on water quality across an urbanized watershed in Bentong, Malaysia. *Ecol. Indic.* **2021**, *122*, 107254. [CrossRef]
29. Le, C.T.U.; Paul, W.L.; Gawne, B.; Suter, P.J. Quantitative Flow-Ecology Relationships Using Distributed Lag Nonlinear Models: Large Floods in the Murray River Could Have Delayed Effects on Aquatic Macroinvertebrates Lasting More Than Three Decades. *Water Resour. Res.* **2020**, *56*, e2019WR025896. [CrossRef]
30. Danehy, R.J.; Bilby, R.E.; Langshaw, R.B.; Evans, D.M.; Turner, T.R.; Floyd, W.C.; Schoenholtz, S.H.; Duke, S.D. Biological and water quality responses to hydrologic disturbances in third-order forested streams. *Ecohydrology* **2012**, *5*, 90–98. [CrossRef]
31. Que, Z.; Wang, X.; Liu, T.; Wu, S.; He, Y.; Zhou, T.; Yu, L.; Qing, Z.; Chen, H.; Yuan, X. Watershed land use change indirectly dominated the spatial variations of CH_4 and N_2O emissions from two small suburban rivers. *J. Hydrol.* **2023**, *619*, 129357. [CrossRef]
32. Tang, H.; Lai, Y.; Zhan, C.; Lu, Z.; Ran, Q. Spatiotemporal changes of the water conservation function in the six major river basins in Yunnan Province, Southwest China. *J. Hydrol. Reg. Stud.* **2026**, *63*, 103073. [CrossRef]
33. He, Y.P.; Xie, H.; Cui, P.; Wei, F.Q.; Zhong, D.L.; Gardner, J.S. GIS-based hazard mapping and zonation of debris flows in Xiaojiang Basin, southwestern China. *Environ. Geol.* **2003**, *45*, 286–293. [CrossRef]
34. Chai, Z.X.; Fan, J.R. Strong erosion and formations in lower reaches of Jinsha River. *J. Soil. Water Conserv.* **2001**, *15*, 14–17. [CrossRef]
35. Yu, G.A.; Huang, H.Q.; Wang, Z.Y.; Brierley, G.; Zhang, K. Rehabilitation of a debris-flow prone mountain stream in southwestern China—Strategies, effects and implications. *J. Hydrol.* **2012**, *414*, 231–243. [CrossRef]
36. Liu, C.L.; Lin, L.J.; Song, C. The impact of land use on CO2 intake of chemical weathering in a typical karst region: A case study of Xiaojiang watershed, Yunnan Province. *Geol. China* **2011**, *38*, 479–488.
37. Zhang, X.H.; Gan, S.; Yuan, X.P. Analysis of land use patterns of debris flow fans in Xiaojiang River Basin of Yunnan Province. *J. Yunnan Univ. Nat. Sci. Ed.* **2020**, *42*, 499–506.
38. Qin, R.J.; Wu, H.; Guo, Q. Investigation of damage situation of the natural landform along Lijiang River based on GIS and RS. *Remote Sens. Land. Resour.* **2013**, *25*, 160–164.
39. Wang, C.Q.; Yan, J.Y.; Li, G.H. Evolution and optimization research on landscape pattern of Yongding River section of Beijing based on ENVI technology. *J. Beijing For. Univ.* **2021**, *43*, 118–129.
40. Lai, Y.H.; Tang, H.L.; Zhan, C.; Hong, S.B.; Ran, Q.H. Evaluating the cumulative and time-lag effects of vegetation response to drought in the Lancang-Mekong River basin. *Ecol. Indic.* **2025**, *178*, 114113. [CrossRef]
41. Chen, A.; Yang, X.; Guo, J.; Zhang, M.; Xing, X.; Yang, D.; Xu, B.; Jiang, L. Dynamic of land use, landscape, and their impact on ecological quality in the northern sand-prevention belt of China. *J. Environ. Manag.* **2022**, *317*, 115351. [CrossRef] [PubMed]
42. Jiang, P.; Wen, C.; Ma, Z.; Dai, F. Spatiotemporal dynamics and planning responses to address carbon balance and land-use mixtures in megacities: A case study of Wuhan, China. *Environ. Impact Assess. Rev.* **2026**, *116*, 108139. [CrossRef]
43. McGarigal, K. *FRAGSTATS Help*; University of Massachusetts: Amherst, MA, USA, 2015; Volume 182.
44. Yu, H.; Hu, X.; Yao, L. Vegetation restoration reduces landscape ecological risk in the Loess Plateau. *Geogr. Sustain.* **2025**, *6*, 100320. [CrossRef]

45. Zhu, A.P.; Yuan, S.Y.; Wen, S.S. Effects of landscape pattern on water quality at multi-spatial scales in the Liuxi River. *Acta Ecol. Sin.* **2023**, *43*, 1485–1495. [CrossRef]
46. Lu, J.G.; Fu, Y.M.; Zhou, Y.; Zhang, L.W.; Shi, X.L. Response of Water Quality to Land Use and Landscape Pattern in the Ganjiang River Watershed. *Environ. Manag.* **2025**, *75*, 155–166. [CrossRef]
47. Fang, Z.J.; Fang, R.J.; Xu, B.L.; Xue, P.W.; Zou, C.L.; Huang, J.H.; Xu, Q.X.; Dai, J.F. Scale Effects of Landscape Patterns on Nitrogen and Phosphorus Pollution in Yanshan River Basin, Guilin, China. *Water* **2024**, *16*, 2472. [CrossRef]
48. Mei, K.; Shi, H.N.; Wu, Y.P.; Dahlgren, R.A.; Ji, X.L.; Yang, M.M.; Guan, Y.R. Impact of landscape patterns on river water quality: Spatial-scale effects across an agricultural-urban interface. *Ecol. Indic.* **2025**, *170*, 113019. [CrossRef]
49. Pei, W.; Xu, Q.Y.; Lei, Q.L.; Du, X.Z.; Luo, J.F.; Qiu, W.W.; An, M.Y.; Zhang, T.P.; Liu, H.B. Interactive impact of landscape composition and configuration on river water quality under different spatial and seasonal scales. *Sci. Total Environ.* **2024**, *950*, 175027. [CrossRef]
50. Dow, C.L.; Arscott, D.B.; Newbold, J.D. Relating major ions and nutrients to watershed conditions across a mixed-use, water-supply watershed. *J. North Am. Benthol. Soc.* **2006**, *25*, 887–911. [CrossRef]
51. Wu, J.H.; Lu, J. Spatial scale effects of landscape metrics on stream water quality and their seasonal changes. *Water Res.* **2021**, *191*, 116811. [CrossRef]
52. Dou, J.; Xia, R.; Chen, Y.; Chen, X.; Cheng, B.; Zhang, K.; Yang, C. Mixed spatial scale effects of landscape structure on water quality in the Yellow River. *J. Clean. Prod.* **2022**, *368*, 133008. [CrossRef]
53. Wang, Y.J.; Fu, G.S.; Jiang, C.J. Analysis on temporal and spatial variation characteristics of water quality in Lixiahe abdominal area, Jiangsu Province. *Yangtze River* **2020**, *51*, 68–73. [CrossRef]
54. Zhu, P.H.; Pan, B.Z.; Li, Z.W.; Zhao, G.N.; Liu, X.Y. Debris flow weakens the ecological role of river microhabitat heterogeneity in mountainous regions. *Ecol. Indic.* **2023**, *153*, 110469. [CrossRef]
55. Li, J.; Wang, G.; Song, C.; Sun, S.; Ma, J.; Wang, Y.; Guo, L.; Li, D. Recent intensified erosion and massive sediment deposition in Tibetan Plateau rivers. *Nat. Commun.* **2024**, *15*, 722. [CrossRef]
56. Zhou, Y.; Wang, J.; Zhou, L.; Zhi, W.; Zhang, Y.; Qin, B.; Wu, F.; Woolway, R.I.; Jane, S.F.; Jeppesen, E.; et al. Episodic flooding causes sudden deoxygenation shocks in human-dominated rivers. *Nat. Commun.* **2025**, *16*, 6865. [CrossRef]
57. Bao, J.; Wang, J.; Xu, W.; Zhang, Z.; Datry, T.; Gomez-Gener, L.; Chen, X.; Zhang, J.; Li, J.; McDowell, W.H.; et al. Intermittent rivers in peri-urban areas act as significant but overlooked sources of N_2O emissions. *Water Res.* **2026**, *288*, 124775. [CrossRef]
58. Pang, Q.; Zhao, G.; Wang, D.; Zhu, X.; Xie, L.; Zuo, D.; Wang, L.; Tian, L.; Peng, F.; Xu, B.; et al. Water periods impact the structure and metabolic potential of the nitrogen-cycling microbial communities in rivers of arid and semi-arid regions. *Water Res.* **2024**, *267*, 122472. [CrossRef]
59. Xin, Y.; Gao, Q.; Zhang, S.; Zhang, Z.; Wang, J.; Xia, X. Microbial regulatory mechanisms underlying methane emission in rivers with different land covers. *Water Res.* **2025**, *281*, 123680. [CrossRef]
60. Zhou, X.Q.; Shen, Y.M.; Tang, J. Numerical modeling of water diversion impacts on water quality improvement in Lake Dianchi. *Environ. Model. Softw.* **2025**, *187*, 106375. [CrossRef]
61. Sun, W.C.; Wang, X.Y.; Ning, Z.; Sun, L.; Wang, S.W. Analysis of Pathogen-Microbiota Indicator Responses in Surface Karst Springs under Various Conditions in a Rocky Desertification Area: A Case Study of the Xiaojiang Watershed in Yunnan. *Appl. Sci.* **2024**, *14*, 1933. [CrossRef]
62. Li, S.K.; He, W.X.; Wang, L.; Zhang, Z.; Chen, X.Q.; Lei, T.C.; Wang, S.J.; Wang, Z.Z. Optimization of landscape pattern in China Luojiang Xiaoxi basin based on landscape ecological risk assessment. *Ecol. Indic.* **2023**, *146*, 109887. [CrossRef]
63. Cai, K. Reflections on the Sources of Total Phosphorus Pollution and Pollution Prevention and Control in the Xiaojiang River Basin of Dongchuan District. *Intell. City* **2020**, *6*, 114–115. [CrossRef]
64. Jiang, X.; She, D.; Huang, X.; Pan, Y.; Xia, Y. Improving water quality prediction through landscape patterns in Euclidean distance-based drainage areas for plain river networks. *J. Hydrol.* **2026**, *669*, 135089. [CrossRef]
65. Wang, Y.; Liu, X.; Wang, T.; Zhang, X.; Feng, Y.; Yang, G.; Zhen, W. Relating land-use/land-cover patterns to water quality in watersheds based on the structural equation modeling. *Catena* **2021**, *206*, 105566. [CrossRef]
66. Yi, M.; Jin, X.; Zhang, H.; Xia, X.; Li, Y. Decoupling of Biodiversity and Network Stability in Sediment-Laden Rivers: A Cross-Regional Analysis of Multitrophic Communities in the Yellow River. *Environ. Sci. Technol.* **2026**, *60*, 1660–1673. [CrossRef]
67. Wang, A.; Yang, D.; Tang, L. Spatiotemporal variation in nitrogen loads and their impacts on river water quality in the upper Yangtze River basin. *J. Hydrol.* **2020**, *590*, 125487. [CrossRef]
68. Wu, Y.; Wang, J.; Liu, Z.; Li, C.; Niu, Y.; Jiang, X. Seasonal nitrate input drives the spatiotemporal variability of regional surface water-groundwater interactions, nitrate sources and transformations. *J. Hydrol.* **2025**, *655*, 132973. [CrossRef]
69. Zhao, H.; Liu, X.; Du, X.; Lei, Q.; Liu, H. Impacts of storm events on watershed phosphorus critical source area identification based on SWAT model. *J. Hydrol.* **2026**, *668*, 135032. [CrossRef]

70. Lou, S.; Zhang, Z.; Zhou, F.; Wang, H.; Zou, Y.; Fedorova, I.V.; Liu, S. Distributions and influencing factors of heavy metals in the coastal areas of the Yangtze River Estuary, China. *Reg. Stud. Mar. Sci.* **2025**, *86*, 104216. [CrossRef]
71. Zhao, Y.; Han, J.; Zhang, B.; Gong, J. Impact of transferred water on the hydrochemistry and water quality of surface water and groundwater in Baiyangdian Lake, North China. *Geosci. Front.* **2021**, *12*, 101086. [CrossRef]

Disclaimer/Publisher's Note: The statements, opinions and data contained in all publications are solely those of the individual author(s) and contributor(s) and not of MDPI and/or the editor(s). MDPI and/or the editor(s) disclaim responsibility for any injury to people or property resulting from any ideas, methods, instructions or products referred to in the content.